

Formulation, Optimization, Characterization, and In Vivo Antidiabetic Evaluation of Bioactive Loaded Polymeric Nanoparticles Incorporated into Topical Nanogel in STZ-Induced Diabetic Rats

Mohit Nagar^{1*}, Ajay Pal Singh², Sanjar Alam³

¹*School of Pharmacy, Lingaya's Vidyapeeth (A Deemed-to-be-University), Nachauli, Jasana Road, Faridabad, Haryana, India.*

²*School of Pharmacy, Lingaya's Vidyapeeth (A Deemed-to-be-University), Nachauli, Jasana Road, Faridabad, Haryana, India.*

³*R. V. Northland Institute of Pharmacy, Dadri, G. B. Nagar, Uttar Pradesh, India.*

Corresponding author:

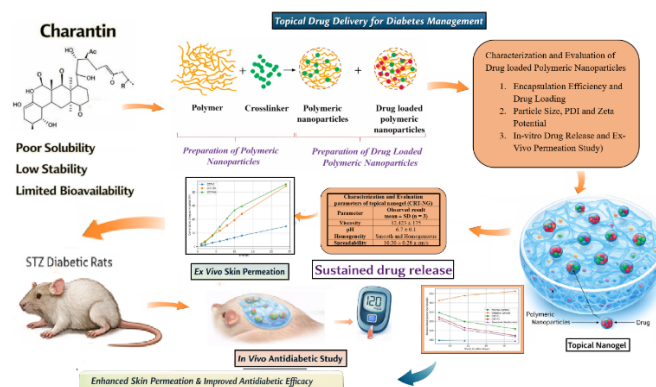
Mohit Nagar

Research Scholar, School of Pharmacy, Lingaya's Vidyapeeth (A Deemed-to-be-University), Nachauli, Jasana Road, Faridabad, Haryana, India. E-mail: nagamohit00@gmail.com

Abstract: Diabetes mellitus is a persistent endocrine disorder in which impaired insulin secretion or action leads to elevated circulating glucose levels. Charantin, a major antidiabetic phytoconstituent of *Momordica charantia*, exhibits strong hypoglycemic activity but is limited aqueous solubility and low oral bioavailability. This study aimed to development, formulate and evaluate charantin-loaded polymeric nanoparticles incorporated into a topical nanogel to enhance topical delivery and antidiabetic efficacy. Polymeric nanoparticles were formulated by ionic gelation and optimized for desirable physicochemical properties. The optimized polymeric nanoparticle formulation (CRT-2A) showed a particle droplet size- 200 ± 0.3 nm, PDI- 0.053 ± 0.03 , and zeta potential -24.0 ± 1.4 mV, indicating uniformity and stability. Encapsulation efficiency was $88.4 \pm 2.7\%$, drug loading $31.84 \pm 0.61\%$, with 92% in-vitro release and 88.92% ex-vivo permeation over 24 hours. Optimized formulation (CRT-2A) was integrated into a 1% Carbopol 938 solution and convert into nanogel (CRT-NG) exhibiting suitable pH (6.7 ± 0.1), viscosity ($12,423 \pm 75$ cps), good spread-ability (10.30 ± 0.8 g·cm/s), and smooth homogeneity, indicating excellent consistency, suitability and ideal used for topical delivery. The optimized formulation (CRT-NG) exhibited First-order release kinetics with a diffusion-controlled mechanism, and ex-vivo studies showed a 2.86-fold enhancement in skin permeation compared to the pure charantin gel. In STZ-induced diabetic rats, CRT-NG (25 and 50 mg/kg) significantly improved glycemic control and glucose tolerance compared to diabetic controls ($p < 0.05$). High and low-dose of drug loaded nanogel treatments showed antidiabetic effects of comparable to metformin. Overall, charantin-loaded polymeric nanoparticle topical nanogel showed enhanced skin permeation, sustained drug release, and improved antidiabetic efficacy, highlighting its potential as a promising transdermal delivery system for effective diabetes management.

Keywords: Polymeric Nanoparticle, Charantin, Diabetes Mellitus, STZ-induced rats, Topical Gel, Antidiabetic Activity.

Graphical Abstract:



*Author for Correspondence: Mohit Nagar

How to cite this article: Mohit Nagar, Ajay Pal Singh, Sanjar Alam.: Formulation, Optimization, Characterization, and In Vivo Antidiabetic Evaluation of Bioactive Loaded Polymeric Nanoparticles Incorporated into Topical Nanogel in STZ-Induced Diabetic Rats..Int J Drug Deliv Technol. 2026; 16(8s): 504-517; DOI: 10.25258/ijddt.16.8s.62

Source of support: Nil.

Conflict of interest: None

INTRODUCTION

Diabetic mellitus is one of the third fast-growing non-communicable disease in all over the world, this disease affecting an estimated 537 million adult peoples in the 2021 and projections reaching 643 million by 2030. (1) Diabetic mellitus is a chronic hyperglycemia condition due to impaired insulin secretion and action or both. Diabetic Mellitus leads to multiple serious complications including retinopathy, nephropathy, neuropathy, cardiovascular diseases, and impaired wound healing. (2) Several synthetic antidiabetic agents such as biguanides, DPP-4 blockers, GLP-1 receptor agonists, sulfonylureas, and insulin therapies are easily accessible, many different kinds of prohibitions also remain. (3) The adverse effect which include hypoglycemia and gastrointestinal intolerance and weight gain and secondary drug resistance together with poor patient compliance. (4) The exploration of herbal drugs for management of diabetes has gained renewed attention because these drugs produce safe results and they can treat multiple diabetic symptoms. (5) *Momordica charantia* (bitter melon) demonstrates strong hypoglycemic effects which establish its medicinal value among various medicinal plants. (6) Bitter melon serves as a traditional vegetable and herbal medicine which contains multiple bioactive compounds including alkaloids, flavonoids, peptides and steroidal saponins. (7) The principle hypoglycemic agent characterizing charantin consist of a mixture which includes sitosterol and stigmasterol glucosides. (8) Charantin produces antidiabetic effects through of its capacity to increase glucose absorption and boost insulin production together with its ability to regulate carbohydrates metabolism enzymes while safeguarding pancreatic beta cells form oxidation damage. (9) The substance enhances lipid processing while decreasing experimental models' glycosylated hemoglobin levels. The therapeutic potential of charantin faces major barriers because its low water solubility, gastrointestinal instability, rapid metabolic breakdown and poor absorption, which prevent its medical application. The administration of higher doses becomes necessary to obtain therapeutic effectiveness which creates risks for safety and treatment adherence. (10) Nano-technology has been recognized as a potentially creative strategy in the delivery of drugs, capable of enhancing solubility, stability, and bioavailability of poorly water-soluble phytoconstituents. (11) Polymeric nanoparticles, particularly those that are based on biodegradable

polymers like chitosan, PLGA, have been highly desirable for their biocompatibility, regulated release behavior, and protection of unstable drugs from degradation. (12-13) Encapsulation of phytochemicals in polymeric carriers enhances their pharmacokinetic profile and therapeutic efficacy, as demonstrated in various preclinical studies. (14) Multiple bioactive constitutes such as lutein, catechin, mangiferin and berberine have been successfully delivered via polymeric nanoparticles, exhibiting enhanced antidiabetic efficacy Comparing with naturally occurring compounds. (15) For example, lutein, catechin, mangiferin, curcumin, quercetin, and berberine-loaded polymeric nanoparticles improved oral bioavailability and glucose-lowering potential in diabetic rats. Similarly, resveratrol nanoparticles protected pancreatic tissue and improved insulin sensitivity. However, limited studies are available on nano-based delivery of charantin, despite its high therapeutic promise. Considering the pharmacological significance of charantin and the limitations associated with its delivery, The goal of the current study was to create bioactive loaded polymeric nanoparticles with chitosan as a carrier, describe their physicochemical characteristics, and assess their potential to prevent diabetes in vivo in rats with STZ-induced diabetes. A potential phytopharmaceutical strategy for the treatment of diabetes is the development of bioactive loaded polymeric nanoparticle-based nanogel for topical application.

Materials and Method

2.1 Chemical and Excipients:

Charantin (CRT) [assayed 99%] was purchased from Sigma-Aldrich Chemicals, Bangalore. Chitosan (medium molecular weight, deacetylation degree $\geq 75\%$), sodium tripolyphosphate (TPP) and Carbopol-938 (Carbomer 938) was purchased from CDH (New Delhi). Tween 20, Potassium di-hydrogen phosphate, methanol, sodium hydroxide and Streptozotocin was procured from Chemical storehouse Facility in R.V. Northland Institute, Greater Noida. Rat skin and cellophane tubes was procured from the Animal House Facility and Pharmacology Research Lab at R.V. Northland Institute in Greater Noida. All chemical, polymer, and reagent used throughout the current study was of analytical quality.

Formulation Development:

Preparation and Development of Placebo Polymeric Nanoparticles by Ion Gelation Method:

Chitosan was selected as the mucoadhesive matrix for the development of polymeric nanoparticle formulations. (16) Placebo polymeric nanoparticles (PNPs) were prepared using varying concentrations of chitosan (1.0–3.0 mg/mL) and sodium tripolyphosphate (TPP, 1.0–3.0 mg/mL) by the ion gelation method. Dropwise TPP solution was added into the chitosan solution, which was continuously magnetically stirred at 1000 rpm at room temperature for a period of 30 minutes. The resulting dispersions were visually examined for the formation of a distinct polymeric nanoparticle system, as summarized in Table 1, and evaluated for clarity, opalescence, precipitation, milky appearance, and aggregation. Placebo PNP formulations exhibiting stable, homogeneous opalescent dispersions without visible precipitation or aggregates were selected for further development of drug-loaded polymeric nanoparticles formulations.

Preparation and Development of Drug loaded Polymeric Nanoparticles: Drug loaded formulations were prepared using the ionic gelation method. The drug was mixed in to chitosan solution at pre-determined concentration based on the optimization on placebo formulation, using polymer-to-drug ratios of 1:1, 1:2, and 1:3, and then sodium tri-poly phosphate (TPP) was added. We gradually added the TPP solution while keeping the mixture stirred with a magnetic stirrer at 1000 rpm for 30 minutes, allowing the polymeric nanoparticle to form at room temperature.

Characterization and Evaluation of Drug Loaded formulation:

Particle Size, PDI and Zeta Potential Determination: The particle size, Polydispersity index (PDI) and zeta potential of the optimized drug loaded formulations were analyzed by using dynamic light scattering (DLS) based on the laser light scattering technique. Measurements were carried out with a -photon correlation spectrometer (Zetasizer Nano S90, Malvern Instruments, Malvern, UK) to evaluate the size distribution and surface charge characteristics of formulations.

In vitro release study: The in vitro release profile of the optimized drug-loaded formulations was determined by dialysis-bag diffusion technique. (17) The dialysis membrane with a molecular weight cut-off (MWCO) of 12,000 Da and a penetration depth of 2.0 nm was employed for the study.

Preparation of Membrane

Prior to experimentation, the dialysis membrane was activated by immersing it in phosphate buffer system (pH 7.2) for 12–24 hours to ensure hydration and removal of preservative residues. The membrane was then rinsed with distilled water and carefully examined for any physical damage. For storage, the hydrated membrane was wrapped in aluminum foil and kept at room temperature overnight until further use.

Release Study Protocol

For the release study, 10 ml of the optimized formulation was placed in a pre-activated dialysis bag and securely sealed within the basket of a USP dissolution apparatus. The basket was immersed in 500 ml of phosphate buffer (pH 7.2) containing 0.1% w/v Tween-20 and maintained at 37 ± 0.5 °C with continuous stirring at 60 rpm. Samples were withdrawn at predetermined intervals of (1-24 h) and replaced with an equal volume of fresh medium to maintain sink conditions. Drug release was quantified using UV-Visible spectrophotometry at 278 nm and cumulative drug release was calculated.

Ex vivo Permeation Studies: The ex-vivo permeation study was conducted using static Franz diffusion cells to evaluate the permeation behavior of the optimized drug loaded formulations. (18) This diffusion cell consisted of donor and receptor compartments separated by excised rat skin. Male albino rats (body weight: 200 ± 20 g) were procured from the Animal House Facility of RVNI, Dadri, Uttar Pradesh, India (Ethical Approval No.: RVNI/IAEC/24-25/02/12) and experiments were conducted in accordance with CPCSEA guidelines. Freshly excised abdominal skin was carefully shaved using an electric shaver. Subcutaneous fat and adhered connective tissues were gently removed. The prepared skin was mounted between the donor and receptor compartments with the stratum corneum facing the donor side. The receptor chamber (20 ml capacity) was filled with phosphate buffer system (pH 7.2), maintained at 37 ± 2 °C, and stirred continuously at 1000 rpm using a magnetic bead to maintain uniformity, while the donor compartment contains the optimized formulation. At predetermined intervals (1-24 hrs), 1 ml sample were withdrawn from the receptor medium and immediately replaced with an equal volume of fresh buffer system to maintain constant receiver conditions. The collected samples were analyzed for drug content using a validated HPLC method at detection wavelength of 278 nm.

Calculation of Permeation Parameters: The steady-state flux (J_{ss}) was determined from the slope of the linear portion of the cumulative permeation versus time

Table.1: Distinct System of Polymeric Nanoparticle

Sr. No.	Distinct system	Visual Observations
1.	Aggregates	formation of visible clumps due to excess crosslinking
2.	Opalescent suspensions	stable colloidal dispersions, indicative of nanoparticles in the nanometer size range.
3.	Clear solutions	absence of nanoparticles, suggesting insufficient crosslinking.

profile using the equation of $J_{ss} = dQ/(A \cdot dt)$. The permeability coefficient (K_p) was calculated as $K_p = J_{ss}/C_0$, where C_0 represents the initial drug concentration in the donor compartment. The enhancement ratio (ER)

was estimated by comparing the flux of the optimized formulation with that of the control ($ER = J_{ss}(\text{formulation})/J_{ss}(\text{control})$).

Preparation, development of nanogel and conventional gel (optimized drug loaded Polymeric Nano particle convert into Topical nanogel):

To improve dermal application compliance, the optimized drug loaded formulation was incorporated into a nanogel using 1% Carbopol 934 as the gelling agent. The optimized drug loaded formulation (equivalent to 0.1 g drug) was then incorporated into the hydrated Carbopol matrix to obtain a homogeneous nanogel (CRT-NG), followed by neutralization with triethanolamine (TEA). A conventional gel was prepared by directly incorporating drug into the Carbopol dispersion and neutralizing with 0.5% w/w TEA, and was designated as the neat formulation conventional gel (CRT-cg).

Characterization of drug loaded polymeric nanoparticle nanogel:

Viscosity and pH Determination: The viscosity and pH determination of optimized nanogel formulation using a cylinder Brookfield viscometer and calibrated digital pH meter.

Homogeneity and Spreadability: The homogeneity of the optimized gel formulation was assessed by gently rubbing a small quantity of gel between the thumb and index finger to evaluate uniformity, smoothness, and the absence of coarse particles, while spread-ability were estimated by the parallel plate method by placing 0.1 g of gel between two glass plates, applying a specified weight, and recording the time required for the gel to spread over a measured distance, expressed as cm/s.

Surface Morphology by TEM (Transmission Electron Microscopy): The surface morphology of the optimized nanogel formulation was characterized by using transmission electron microscopy (TEM, JEOL/JEM-2100, Japan). A diluted sample placed into a carbon-coated copper grid, excess liquid was removed, and the specimen was negatively stained with 1% phosphotungstic acid. After air drying, image was captured at different magnifications under an accelerating voltage of 200 kV.

In-vitro kinetic study: The in-vitro kinetics release of the optimized formulation (CRT-NG) were evaluated using a Franz diffusion cell. The donor compartment contained 0.5 g of nanogel, while the receptor compartment was filled with 20 mL phosphate buffer system (pH 7.2), maintained at 37 ± 0.5 °C under continuous stirring at 1000 rpm. At predetermined intervals (1, 24 hrs), 1 ml sample were withdrawn and replaced with fresh PBS to maintain sink conditions. The drug content was quantified using UV spectrophotometry at 278 nm. The release data were fitted to zero-order, first-order, Higuchi, and Korsmeyer-Peppas model using regression analysis.

Stability Studies: The optimized formulation (CRT-NG) was tested according to accelerated stability testing as per ICH/WHO standards. Formulated samples were stored in three sealed packs at 40 ± 5 °C and $75 \pm 5\%$ RH (Relative Humidity) for a period of 90 days. At predetermined intervals (0-90 days), samples were withdrawn and analyzed. (19) The samples were diluted with methanol, filtered, and assayed for drug content using a validated HPLC method. In addition, the physical characteristics of the formulation (appearance, clarity, phase separation, and consistency) were monitored, and in vitro drug release studies were conducted to assess performance stability.

Comparative Ex vivo Permeation Study: Comparative ex-vivo skin permeation studies were carried out using Franz diffusion cells with excised Wistar rat skin mounted between the donor and receptor compartments. (20) A comparative permeation evaluation was performed for the optimized drug-loaded polymeric nanoparticle formulation, the topical nanogel, and the drug-loaded conventional gel.

In Vivo Antidiabetic Evaluation: The Wistar rats (180–220 g) were maintained according to standard laboratory conditions with an unlimited access to both water and food, and all experimental procedures were approved by the Institutional Animal Ethics Committee (IACE), Animal House Facility of R V Northland Institute, Dadri, Uttar Pradesh, India (Ethical Approval No.: RVNI/IAEC/24-25/02/12). The disease was induced through an intraperitoneal injection of streptozotocin (55 mg/kg) diluted in citrate buffer (pH 4.5), and rats with blood glucose levels >250 mg/dL after 72 h proved to be diabetic. (21) Animals were randomly divided into six groups (n = 6): normal control (vehicle), diabetic-control (STZ), diabetic rats treated with CRT-NG (low dose), diabetic rats treated with CRT-NG (high dose), and a standard treatment group receiving metformin (100 mg/kg, orally). (22) Random blood glucose levels were monitored on days 7, 14, and 28 to evaluate antidiabetic efficacy.

Skin Irritancy Test: The skin irritancy of the optimized formulation CRT-NG was assessed using healthy albino Wistar rats (150–200 g, n=6). A 2 cm² dorsal skin area was shaved 24 h prior to the experiment. (23) About 0.2 g of CRT-NG was applied once daily under non-occlusive conditions. The treated skin site was visually examined at 24 h and 48 h for any signs of redness (erythema) and swelling (edema). The Draize scoring method (0 = no reaction, 1 = minor, 2 = moderate, 3 = severe) was used to grade the severity.

Statistical analysis: The results of this study are represented as mean \pm standard deviation (SD) based on three separate measurements unless specified otherwise. We looked at the results by running a one-way analysis of variance (ANOVA) to evaluate the significant difference were among the different experimental

groups. For the experimental analysis, we relied on GraphPad Prism software, specifically version 5.0. We

considered a result statistically significant if the probability value of $p < 0.05$.

Result and Discussion

Formulation and Development:

Development and Preparation of Placebo Polymeric Nanoparticles:

The based on the result obtained for various concentration of CS and TPP (Table 2), The optimized CS:TPP ratio was identified, as it produced stable, homogeneous and opalescent dispersions without any visible precipitation. These included CS:TPP ratios of 1.5:2.0 mg/mL (MN-2C), 1.75:2.0 mg/mL (MN-3C), and 2.0:2.0 mg/mL (MN-4C). The chosen ratios show that chitosan and TPP are effectively cross-linking, which leads to stable polymeric nanoparticle system that are suitable for drug loaded formulation.

Table.2: Visual Results showing effect of various concentrations of Chitosan (CS) and Tripolyphosphate (TPP).

Formulation code	Con. of CS (mg/ml)	Formulation Sub- code	Con. of TPP (mg/ml)	Visual observation
MN-1	1.0	A	1.0	Clear
		B	1.5	Clear
		C	2.0	Opalescent with ppt
		D	2.5	Opalescent Without ppt
		E	3.0	Opalescent without ppt
MN -2	1.5	A	1.0	Clear
		B	1.5	Clear
		C	2.0	Opalescent without ppt
		D	2.5	Opalescent with ppt
		E	3.0	Aggregates
MN -3	1.75	A	1.0	Clear
		B	1.5	Opalescent without ppt
		C	2.0	Opalescent without ppt
		D	2.5	Opalescent with ppt
		E	3.0	Opalescent with ppt
MN -4	2.0	A	1.0	Clear
		B	1.5	Opalescent without ppt
		C	2.0	Opalescent without ppt
		D	2.5	Milky and aggregates
		E	3.0	Aggregates
MN -5	2.5	A	1.0	Clear
		B	1.5	Clear
		C	2.0	aggregates
		D	2.5	aggregates
		E	3.0	Milky and aggregates
MN-6	3.0	A	1.0	Clear
		B	1.5	Clear
		C	2.0	Opalescent with ppt
		D	2.5	Opalescent with ppt
		E	3.0	Aggregate

Formulation and Development of Drug Loaded Polymeric Nanoparticle:

Three ratios of CS and TPP (1.5:2.0, 1.75:2.0 and 2.0:2.0 mg/ml) was selected for drug loaded formulations on the basis of initial visual optimization study performed during placebo formulation. Such optimized placebo formulation was employed as a base system for preparing for drug loaded formulations. In order to systematically study the effect of polymer concentration on properties of polymeric nanoparticles, the ratio of drug and polymer concentration was varied form 1:1 to 1:3 allowing for evaluation of the impact of increasing amount of drug in drug loaded formulations.

Formulation Code		Volume (ml)		Drug and polymer ratio	Concentration (mg/ml)		
		CS	TPP		CS	TPP	Drug
CRT-1	A	10	04	1:1	1.50	2.0	17.5
	B	10	04	2:1	1.50	2.0	35.0
	C	10	04	3:1	1.50	2.0	52.5
CRT-2	A	10	04	1:1	1.75	1.5	17.5
	B	10	04	2:1	1.75	1.5	35.0
	C	10	04	3:1	1.75	1.5	52.5
CRT-3	A	10	04	1:1	2.0	2.0	17.5
	B	10	04	2:1	2.0	2.0	35.0
	C	10	04	3:1	2.0	2.0	52.5

Optimization, Characterization and Evaluation of Drug Loaded Formulations:

Entrapment Efficiency, Drug Loading, and Percentage Yield: The effect of drug concentration on entrapment efficiency, drug loading, and percentage yield was presented in table 4. All formulations showed satisfactory drug incorporation, with %EE 64.28-89.31 %, %DL 9.12- 31.84% and percentage yield ranged from 72.46-95.40%. CRT-2A having the highest encapsulation, drug loading and yield throughout the batches. CRT-A, CRT-B and CRT-C were selected for further evaluation based on overall performance.

Among the CRT-1 to CRT-3 series, formulations containing higher chitosan concentrations with optimized TPP levels showed superior encapsulation performance. The CRT-2 series demonstrated the best overall results (table. 4). Consequently, CRT-2A, CRT-2B, and CRT-2C were selected for further evaluation.

Formulation Code		Entrapment Efficiency (%)	Drug Loading (%)	Percentage Yield (%)
CRT-1	A	64.28 ± 1.34	9.12 ± 0.28	72.46 ± 1.52
	B	71.63 ± 1.21	13.85 ± 0.36	77.94 ± 1.38
	C	76.92 ± 1.14	17.46 ± 0.41	81.68 ± 1.29
CRT-2	A	93.62 ± 0.88	31.84 ± 0.61	95.60. ± 0.92
	B	88.46 ± 0.94	24.18 ± 0.48	91.82 ± 1.06
	C	74.82 ± 1.12	16.74 ± 0.39	83.68 ± 1.34
CRT-3	A	69.54 ± 1.26	12.18 ± 0.33	78.26 ± 1.44
	B	78.86 ± 1.08	18.92 ± 0.45	84.72 ± 1.22
	C	85.94 ± 0.97	24.86 ± 0.52	± 1.11

Particle Size Determination, Polydispersity Index and Zeta Potential: The particle size, PDI, and zeta potential of the optimized formulations are presented in (Table. 5) and Fig. CRT-2A showed the smallest particle size (200 nm) with a narrow size distribution (PDI 0.053 ± 0.03). CRT-2B and CRT-2C exhibited increased particle sizes (238 nm and 467.5 nm, respectively) with higher PDI values. All formulations possessed a positive zeta potential, indicating good colloidal stability due to chitosan.

Sr. No.	Formulation Code	Particle Size Determination	PDI mean ± SD (n = 3)	Zeta Potential mean ± SD (n = 3)
1.	CRT-2A	200	0.053 ± 0.03	+19.4 ± 1.5
2.	CRT-2B	238	0.420 ± 0.07	+24.2 ± 1.8
3.	CRT-2C	467.5	0.277 ± 0.05	+28.6 ± 1.2

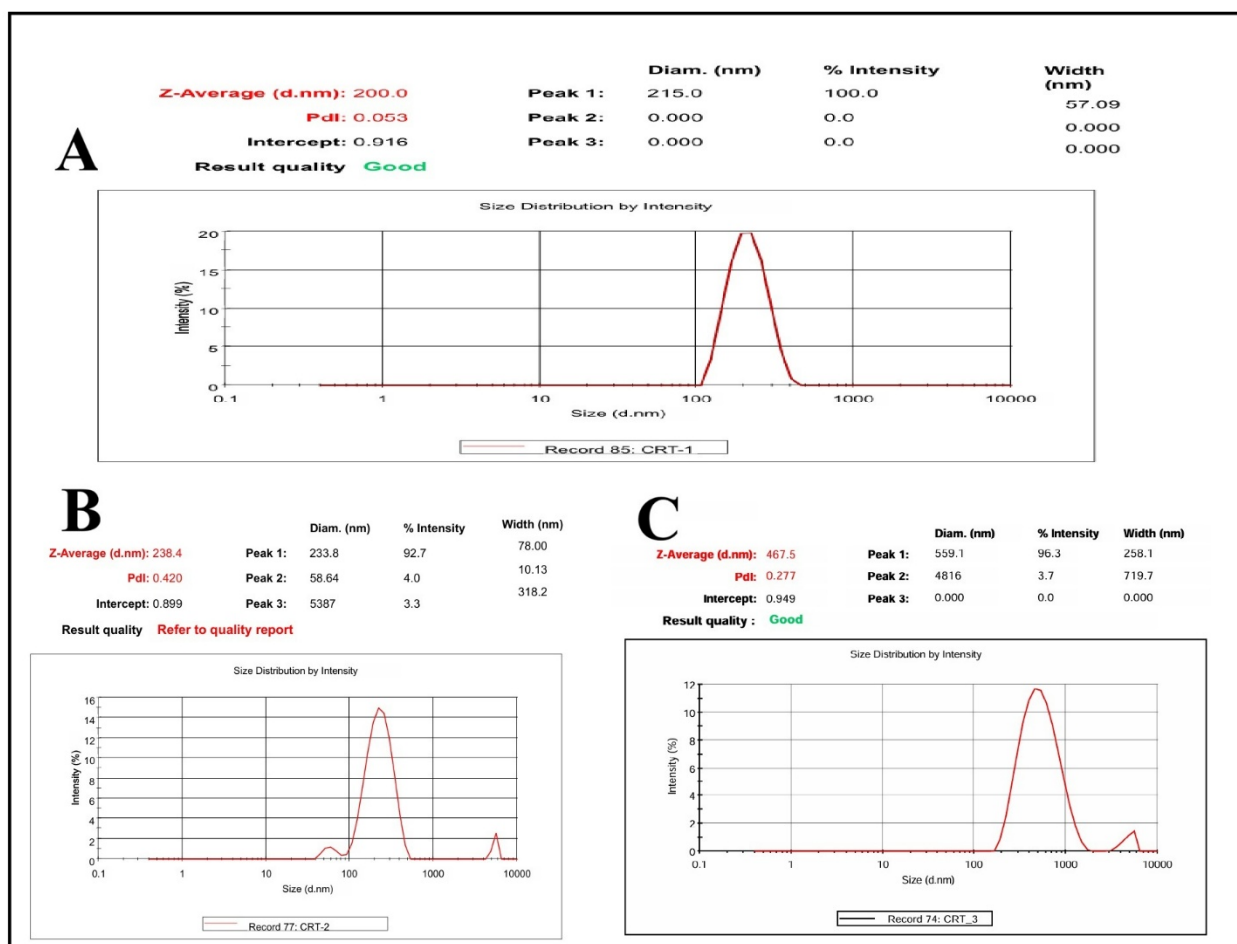


Fig: particle Size determination of optimized drug loaded formulation (CRT-2A, CRT-2B, and CRT-2C)

In vitro release study: The in-vitro release study of drug-loaded optimized formulation (CRT-2A, CRT-2B, and CRT-2C) confirmed their controlled release characteristics, showing a bi-phasic profile with an initial burst in the first 2 h from surface-associated drug, followed by sustained diffusion through the polymeric matrix. Among the formulations, CRT-2A demonstrated superior controlled release (32% at 2 h, 63% at 6 h, and 92% at 24 h), compared with CRT-2B (85% at 24 h) and CRT-2C (77.6% at 24 h).

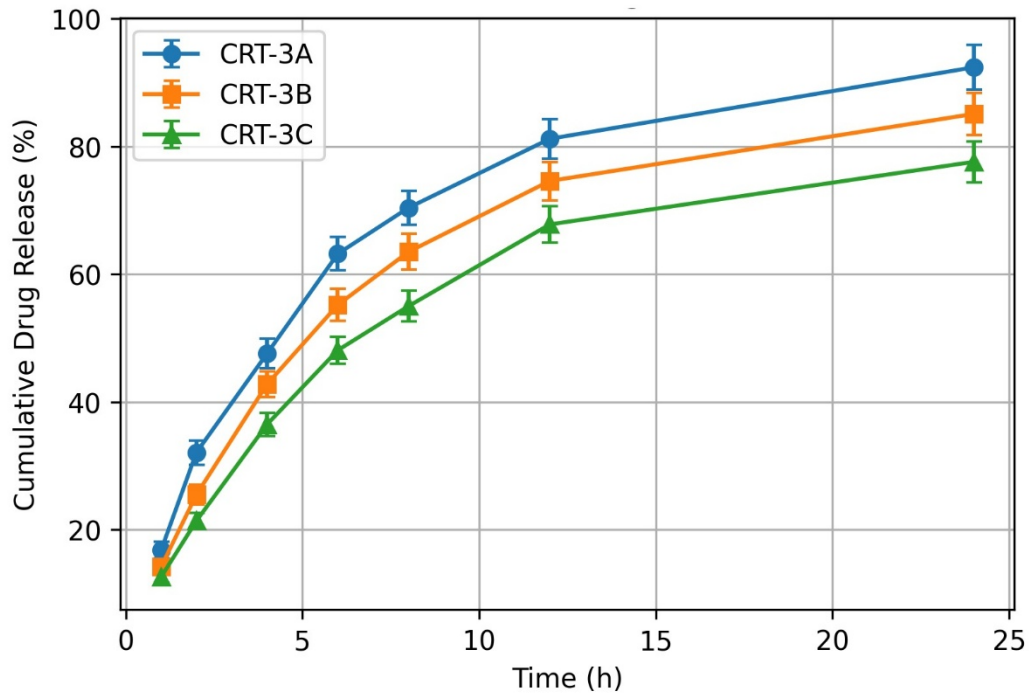


Fig.1: In-vitro % cumulative drug release profile of drug loaded optimized formulations

Ex-vivo Permeation Studies: The ex-vivo permeation study across excised rat skin demonstrated sustained, time-dependent drug diffusion from all optimized formulations. CRT-2A showed the highest cumulative permeation (88.92% at 24 h), followed by CRT-2C (79.56%) and CRT-2B (74.56%). Correspondingly, the steady-state flux (J_{ss}) values were 242.79, 220.81, and 185.40 $\mu\text{g}/\text{cm}^2\cdot\text{h}$ for CRT-2A, CRT-2C, and CRT-2B, respectively, indicating enhanced skin permeation and prolonged therapeutic potential, particularly for CRT-2A.

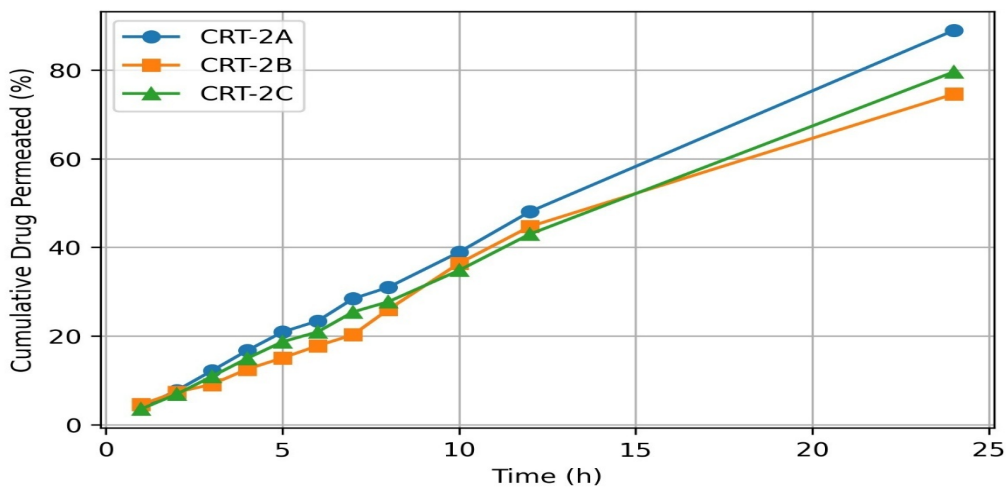


Fig.2: Ex-vivo cumulative drug permeation profile of optimized formulation

Conversion of the Optimized Drug Loaded Formulation into Topical Nanogel: According to the drug loaded formulations physicochemical characterization and performance evaluation of CRT-2A was selected as the optimized formulation and further incorporated into topical nanogel (CRT-NG). The optimized formulation was then added in to hydrogel with 1% Carbopol 934 as a gelling agent to increase suitability in topical delivery and improve patient adherence.

Physicochemical Characterization and Evaluation of topical nanogel:

Determination of Viscosity, pH, Homogeneity and spreadability: The physiochemical characterization of the optimized formulation (CRT-NG), such as viscosity, pH, homogeneity, and spreadability are listed in Table 6. The optimized formulation (CRT-NG) having suitable rheological properties, skin-compatible pH, and good spreadability.

Parameter	Method	Observed result mean \pm SD (n = 3)	Inference
Viscosity	Brookfield viscometer (concentric cylinder)	12,423 \pm 175	Suitable rheology for topical application
pH	Digital pH meter	6.7 \pm 0.1	Skin-compatible
Homogeneity	Visual inspection	Smooth homogeneous,	Uniform nanoparticle distribution
Spreadability	Glass slide method	10.30 \pm 0.28 g.cm/s	Easy application and uniform skin coverage

TEM Morphology: The TEM micrograph of the optimized formulation (CRT-NG) with clear, rounded nanoparticle with smooth surface and even distribution. The aggregation was minimal and the particle size was between about 150 to 250 nm, which is confirmation that the particles were nanoscale stable.

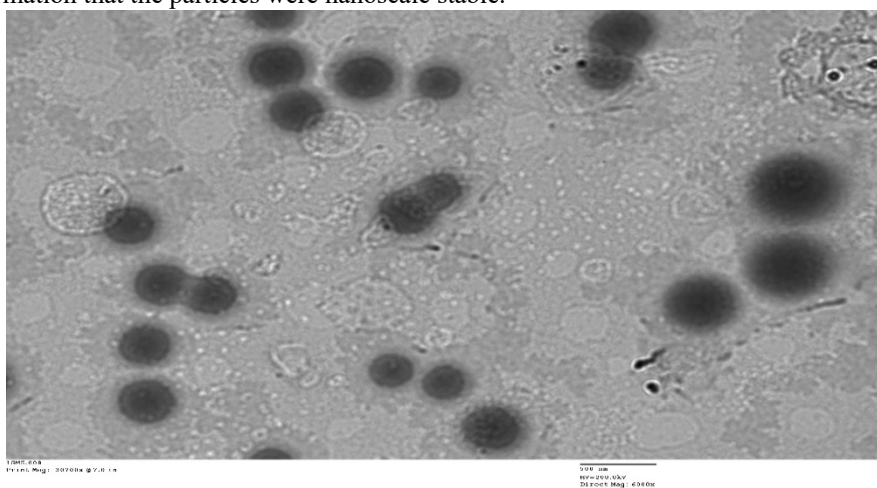


Fig.3: TEM analysis of optimized formulation (CRT-NG)

In-vitro kinetic analysis: The release data of optimized formulation (CRT-NG) was modelled on different kinetic models to determine the drug release mechanism (Table 7 and fig.4). the highest correlation was achieved with the first-order model ($R^2=0.9904$), which implies concentration-dependent release and the rate decreases with time as the drug content decreases. Diffusion-controlled release via the polymeric matrix was also indicated by the good fit of the Higuchi model ($R^2=0.9818$). the zero-order model ($R^2=0.9401$) was not appropriate implying that release does not vary with time. Both relaxation of polymer and diffusion as a super case-II transport mechanism identified in the Korsmeyer peppas model ($R^2=0.9782$). In general CRT-NG shows a stable and regulate release profile.

Sr. No.	Release model	Regression (R^2)	Slope=K
1.	Zero-order	0.9401	3.8527
2.	First-order	0.9904	-0.0414
3.	Higuchi	0.9818	23.429
4.	Korsmeyer peppas	0.9782	1.0682

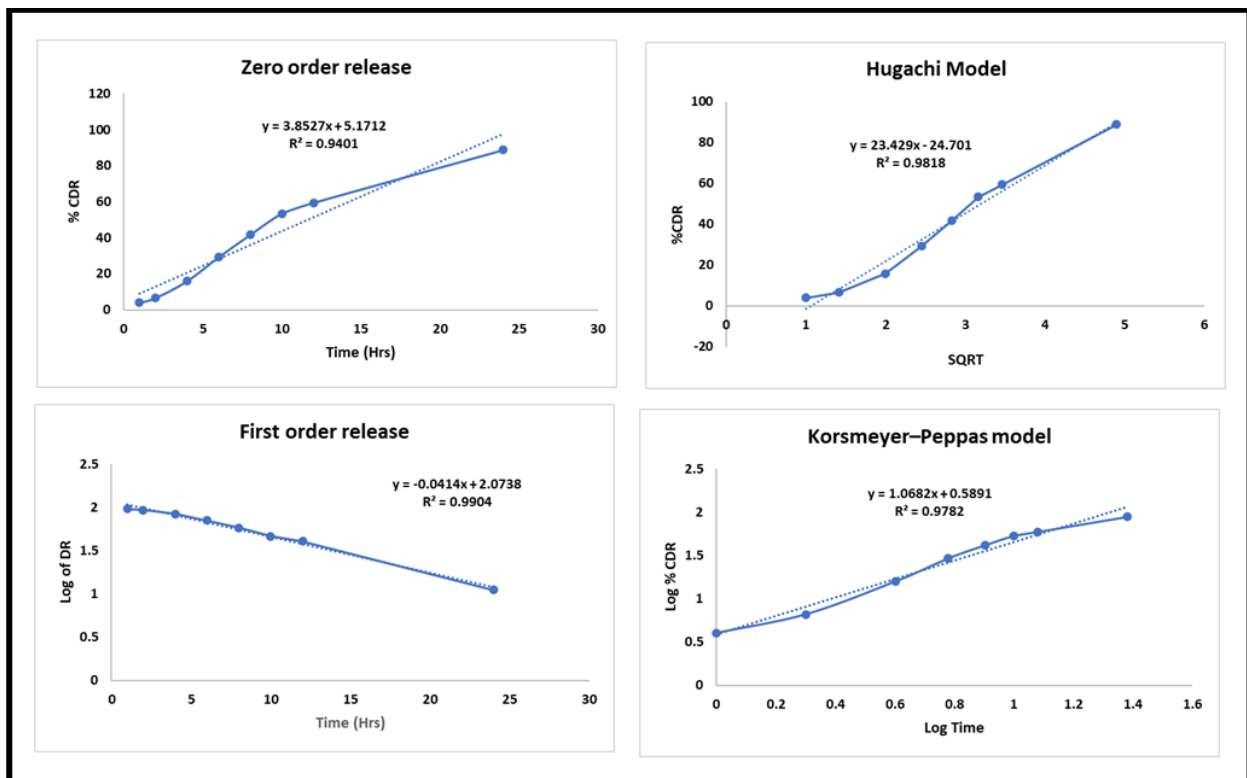


Fig.4: (A - D). Plots of release kinetics: (A) Zero-order, (B) First-Order, (C) Higuchi model, (D) Peppas models for CRT-NG formulation.

Accelerated Stability Studies: The optimized topical nanogel (CRT-NG) was conducted under the guidance of ICH Q1A(R2) to determine the physical, chemical and microbiological stability of the optimized formulation. Samples were incubated in acceleration conditions and samples were analyzed at predetermined time (0-90 days). Samples were stored under accelerated conditions and analyzed at predetermined intervals (0-90 days). The optimized formulation was evaluated regarding appearance, phase separation, consistency, homogeneity, pH, drug content and sterility. The optimized formulation (CRT-NG) was also transparent, homogeneous and smooth, there was no sign of phase separation all through the study. The pH showed only a marginal decrease (6.7 ± 0.1 to 6.5 ± 0.1). The drug content was above 98% which showed little degradation. The formulation was always sterile at predetermined interval. According to the degradation kinetics, the approximate shelf life (T_{90}) was estimated at about 18 months (529 days), which confirms that stability is satisfactory and can be used for clinical purpose.

me (days)	Appearance	Phase separation	Consistency	Homogeneity	pH	Drug Content	Sterility test
0	Clear	None	Smooth	Uniform	6.7 ± 0.1	100 ± 1.2	Sterile
15	Clear	None	Smooth	Uniform	6.7 ± 0.1	99.5 ± 1.4	Sterile
30	Clear	None	Smooth	Uniform	6.7 ± 0.1	99.2 ± 1.3	Sterile
45	Clear	None	Smooth	Uniform	6.7 ± 0.1	98.9 ± 1.5	Sterile

60	Clear	None	Smooth	Uniform	6.6 ± 0.1	98.7 ± 1.2	Sterile
75	Clear	None	Smooth	Uniform	6.6 ± 0.1	98.5 ± 1.4	Sterile
90	Clear	None	Smooth	Uniform	6.5 ± 0.1	98.3 ± 1.5	Sterile

Comparative Ex-Vivo Permeation Study:

Comparative ex-vivo permeation profile of optimized drug loaded polymeric formulation (CRT-2A), drug loaded polymeric nanoparticle topical nano gel (CRT-NG) and drug loaded conventional gel (CRT-G) were studied on static Franz diffusion cells. All formulations exhibited a time-dependent increase in cumulative drug permeation across the membrane. Among the tested formulations, CRT-NG demonstrated the highest cumulative permeation (92.41% at 24 h), followed by the optimized polymeric nanoparticle formulation CRT-2A (88.92%), whereas the conventional gel CuE-G showed markedly lower permeation (29.64%), as shown in Fig. 5. The steady-state flux (Jss), permeability coefficient (Kp), and enhancement ratio (ER) obtained from the comparative ex-vivo permeation study was summarized in Table 9, showing significantly higher permeation for the optimized polymeric nanoparticle compared to the optimized formulation topical nanogel and conventional gel.

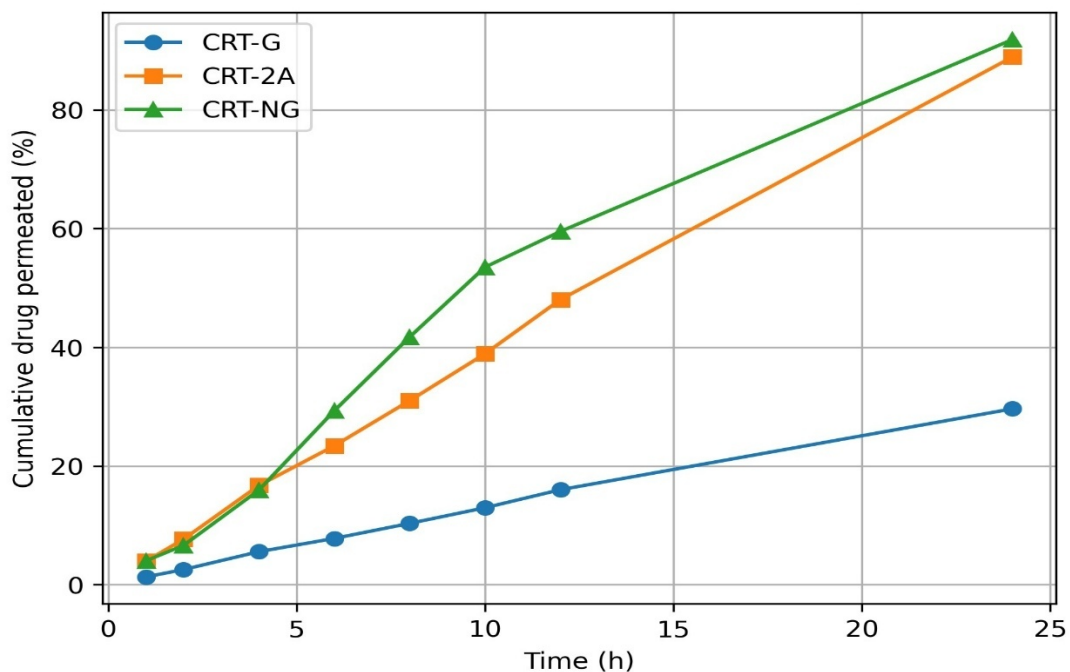


Fig.5: Comparative ex-vivo skin permeation profiles of CRT-G, CRT-2A, and CRT-NG. (CRT-2A: optimized polymeric nanoparticle formulation, CRT-NG: optimized polymeric nanoparticle-loaded topical nanogel, and CRT-G: conventional gel)

Table.9: Comparative ex-vivo permeation parameters of drug loaded formulations mean ± SD (n = 3)			
Formulation	Jss (µg/cm ² ·h)	Kp (cm/h)	ER
CRT-G	80.88 ± 2.94	0.0121 ± 0.0004	-----
CRT-2A	242.64 ± 7.86	0.0364 ± 0.0012	3.00
CRT-NG	231.65 ± 8.12	0.0347 ± 0.0013	2.86
ER calculated with respect to the conventional gel (CuE-G).			

In Vivo Antidiabetic Evaluation:

The effect of CRT-loaded formulations on random blood glucose levels in streptozotocin (STZ)-induced diabetic rats for 28 days are summarized in **Table 10** and **fig.6**. was statistically analyzed, for its hypoglycemic effect and found statistically as compared with standard drug (Metformin) and control group.

Table. 10: Effect of CRT loaded formulations on random blood glucose levels in STZ-induced diabetic rats (mean ± SD (n = 6))

Groups	Treatment	Dose	Random Blood glucose level		
			7 th Day	14 th day	28 th day
I	Control	NA	96.4 ± 6.8	94.2 ± 5.9	92.8 ± 6.1
II	Toxic	55mg/kg	278.6 ± 18.4	338.9 ± 21.6	362.7 ± 24.3
III	Diabetes + CRT-F1	30mg/kg	246.3 ± 15.7	198.4 ± 14.9	158.6 ± 12.8
IV	Diabetes + CRT-F2	60mg/kg	221.5 ± 14.3	164.7 ± 12.6	122.9 ± 10.4
V	Diabetes+ Standard	100mg/kg	210.8 ± 13.9	152.3 ± 11.8	116.4 ± 9.6

Statistical significance:
* p < 0.05, ** p < 0.01 compared with diabetic control (Group II).

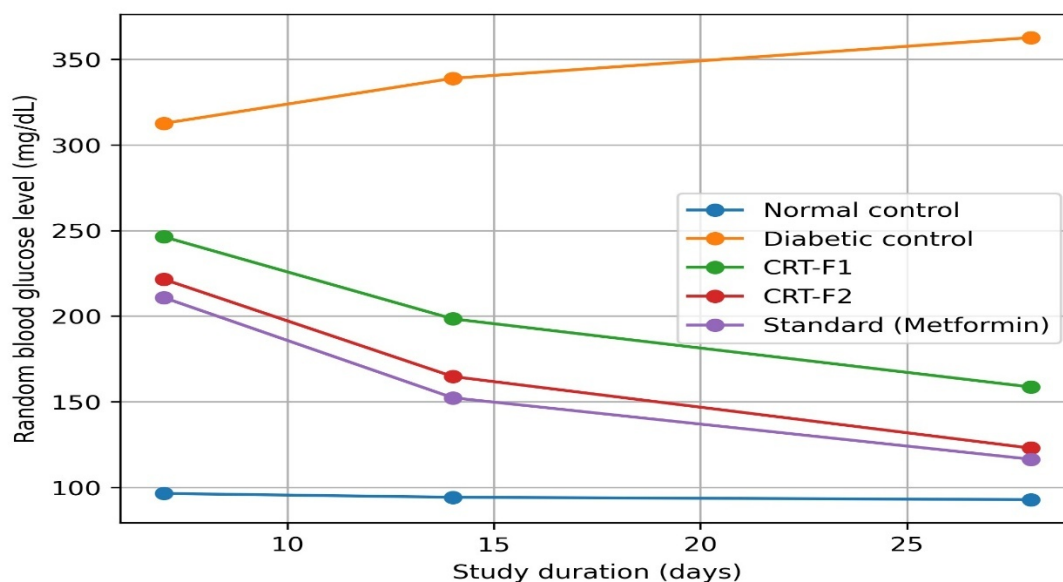


Fig.6: Effect of CRT-loaded formulations on random blood glucose levels in STZ-induced diabetic rats

Skin Irritancy Test: The mean skin irritancy score for the optimized formulation (CRT-NG) was found to be 1.58 in table. 11, which falls within the acceptable non-irritant range. This confirms that the developed formulation is well-tolerated and safe for transdermal application without causing any noticeable erythema or edema.

Table. 11: Skin irritation assessment of optimized CRT-NG formulation

(a) Individual Skin Irritation Scores (A: erythema score; B: oedema score)

Rat	Intact				Abraded			
	24h (A)	24h (B)	72h (A)	72h (B)	24h (A)	24h (B)	72h (A)	72h (B)
1	0	1	0	1	1	1	1	1
2	0	1	1	0	1	1	1	1
3.	1	1	0	1	1	1	1	1

(b) Final Irritation Scores (Total = erythema + oedema; Average = mean of readings)					
Rat	Intact 24h	Intact 72h	Abraded 24h	Abraded 72h	Average Score
1	1	1	2	2	1.5
2	1	1	2	2	1.5
3	2	1	2	2	1.75
Combined Mean Score					1.58

Conclusion:

In conclusion, this study successfully developed and optimized drug loaded polymeric nanoparticle formulation convert in to topical nanogel (CRT-NG) for enhanced topical drug delivery and its antidiabetic efficacy. The optimized polymeric nanoparticles exhibited high entrapment efficiency, drug loading, and percentage yield, along with suitable particle size, narrow PDI, and positive zeta potential, confirming good colloidal stability. In-vitro release and ex-vivo skin permeation studies demonstrated sustained drug release and improved permeation across rat skin.

The polymeric nanoparticle thus optimized, when put into a nanogel, showed suitable pH, homogeneity, spreadability and viscosity, which makes them compatible with skin and easy to use. Notably, In-vivo analysis was showed a substantial drop in random blood glucose level in diabetic rats, which demonstrate effective antidiabetic activity. Overall, the developed drug loaded polymeric nanoparticle, upon incorporation into topical nanogel, represents a promising non-invasive system for sustained and effective topical drug delivery system.

Acknowledgement: The authors gratefully acknowledge Lingaya's Vidyapeeth and R V Northland Institute for providing the necessary facilities and support. We sincerely thank Dr. Ajay pal Singh and Dr. Sanjar Alam for their guidance and encouragement, and the technical staff for their assistance in experimental work.

Conflict of interest: No

Reference:

1. Zhao, Q. and Peng, C., The Global Burden of

Disease Attributable to High Fasting Plasma Glucose in 204 Countries and Territories, 1990–2021: A Systematic Analysis of the Global Burden of Disease Study 2021. *Cheng, The Global Burden of Disease Attributable to High Fasting Plasma Glucose in, 204*, pp.1990-2021.

2. Yameny, A.A., 2025. Diabetes Mellitus: A Comprehensive Review of Types, Pathophysiology, Complications, and Standards of Care in Diabetes 2025. *Journal of Medical and Life Science, 7(1)*, pp.134-141.

3. Cabré, F., Centelles, J.J. and Cascante, M., 2025. From Current Therapeutics to Multitarget Ligands: A Review of Diabetes Pharmacological Treatments. *Pharmaceutics, 17(9)*, p.1125.

4. Chaudhury, A., Duvoor, C., Reddy Dendi, V.S., Kraleti, S., Chada, A., Ravilla, R., Marco, A., Shekhawat, N.S., Montales, M.T., Kuriakose, K. and Sasapu, A., 2017. Clinical review of antidiabetic drugs: implications for type 2 diabetes mellitus management. *Frontiers in endocrinology, 8*, p.6.

5. Khan, M.A. and Siddique, H.R., 2023. The Multi-Targeting Efficacy and Therapeutic Effects of Ayurveda and Chinese Medicine: An Integrated Approach for Cancer Treatment and Management. In *Ethnic Knowledge and Perspectives of Medicinal Plants* (pp. 389-417). Apple Academic Press.

6. Oyelere, S.F., Ajayi, O.H., Ayoade, T.E., Pereira, G.B.S., Owoyemi, B.C.D., Ilesanmi, A.O. and Akinyemi, O.A., 2022. A detailed review on the phytochemical profiles and anti-diabetic mechanisms of *Momordica charantia*. *Heliyon, 8(4)*.

7. Xu, B., Li, Z., Zeng, T., Zhan, J., Wang, S., Ho, C.T. and Li, S., 2022. Bioactives of *Momordica charantia*

as potential anti-diabetic/hypoglycemic agents. *Molecules*, 27(7), p.2175.

8. Desai, S. and Tatke, P., 2015. Charantin: An important lead compound from *Momordica charantia* for the treatment of diabetes. *J Pharmacogn Phytochem*, 3(6), pp.163-166.

9. Nagappan, K., Anoop, K., Kowmudi, G. and Sailaja, M., 2018. Charantin: a neglected antidiabetic compound from *Momordica charantia* L. *Int J Pharm Sci Rev Res*, 51(7), pp.35-40.

10. George, M., Rajkumar, A., Nair, A.K., Vincent, B., VR, C. and Joseph, L., 2025. A Review on Antidiabetic Properties of *Momordica charantia*. *Journal of Pharma Insights and Research*, 3(3), pp.429-437.

11. Chowdhury, S., Nath, D., Chanda Das, S.R., Kar, K., Chakraborty, P., Kapoor, D.U. and Prajapati, B.G., 2024. Nanotechnology based herbal drug delivery system: Current insights and future prospects. *Current Nanomedicine*.

12. Kamaly, N., Yameen, B., Wu, J. and Farokhzad, O.C., 2016. Degradable controlled-release polymers and polymeric nanoparticles: mechanisms of controlling drug release. *Chemical reviews*, 116(4), pp.2602-2663.

13. Beach, M.A., Nayanathara, U., Gao, Y., Zhang, C., Xiong, Y., Wang, Y. and Such, G.K., 2024. Polymeric nanoparticles for drug delivery. *Chemical Reviews*, 124(9), pp.5505-5616.

14. Parvin, N., Aslam, M., Joo, S.W. and Mandal, T.K., 2025. Nano-phytochemistry: harnessing plant-derived phytochemicals in nanocarriers for targeted human health applications. *Molecules*, 30(15), p.3177.

15. Kambale, E.K., Quetin-Leclercq, J., Memvanga, P.B. and Beloqui, A., 2022. An overview of herbal-based antidiabetic drug delivery systems: focus on lipid-and inorganic-based nanoformulations. *Pharmaceutics*, 14(10), p.2135.

16. Alam, S., Khan, Z.I., Mustafa, G., Kumar, M., Islam, F., Bhatnagar, A. and Ahmad, F.J., 2012. Development and evaluation of thymoquinone-encapsulated chitosan nanoparticles for nose-to-brain targeting: a pharmacoscintigraphic study. *International journal of nanomedicine*, pp.5705-5718.

17. Nagar M, Alam S and Rashid M: Preparation, characterization and in-vitro evaluation of berberine loaded nanoemulsion for enhanced antimicrobial efficacy. *Int J Pharm Sci & Res* 2023; 14(4): 1907-20. doi: 10.13040/IJPSR.0975-8232.14(4).1907-20.

18. Patil, A., Jain, G., Iliger, S.R., Nagar, M., Ranjan, N., Kar, S.M., Pawar, S.R. and Rani, M., 2023.

FORMULATION, CHARACTERISATION AND PHARMACOKINETICS OF FELODIPINE NANOVESICLES FOR TRANSDERMAL DRUG DELIVERY SYSTEM. *J Cardiovasc Dis Res*, 14(7), pp.85-105.

19. Nunes, D., Andrade, S., Ramalho, M.J., Loureiro, J.A. and Pereira, M.C., 2022. Polymeric nanoparticles-loaded hydrogels for biomedical applications: A systematic review on in vivo findings. *Polymers*, 14(5), p.1010.

20. Nagar, M., 2023. Review on Nano-Emulsion Drug Delivery System and Formulation, Evaluation and Their Pharmaceutical Applications. *International Journal of Health Care and Nursing*, 2, pp.35-61.

21. Asad, M.I., Khan, D., Rehman, A.U., Elaissari, A. and Ahmed, N., 2021. Development and in vitro/in vivo evaluation of pH-sensitive polymeric nanoparticles loaded hydrogel for the management of psoriasis. *Nanomaterials*, 11(12), p.3433.

22. Singh, K., & Sharma, V. (2024). Development and Characterization of Charantin Loaded Transfersomes based Transdermal Formulation: An Effective and Patient Friendly Way for Diabetes Management. *Journal of Natural Remedies*, 24(3), 629–636.

23. Abdelkader, D.H., Tambuwala, M.M., Mitchell, C.A., Osman, M.A., El-Gizawy, S.A., Faheem, A.M., El-Tanani, M. and McCarron, P.A., 2018. Enhanced cutaneous wound healing in rats following topical delivery of insulin-loaded nanoparticles embedded in poly (vinyl alcohol)-borate hydrogels. *Drug delivery and translational research*, 8(5), pp.1053-1065.